Artifacts in EEG of simultaneous EEG-fMRI: Pulse artifact remainders in the gradient artifact template are a source of artifact residuals after average artifact subtraction

Artifacts in EEG of simultaneous EEG-fMRI: Pulse artifact remainders in the gradient artifact template are a source of artifact residuals after average artifact subtraction

David Steyrl and Gernot R. Müller-Putz*

*Corresponding Author

Gernot R. Müller-Putz
Institute of Neural Engineering, Graz University of Technology
gernot.mueller@tugraz.at

Abstract

Objective: The simultaneous application of electroencephalography (EEG) and functional magnetic resonance imaging (fMRI) opens up new ways to investigate the human brain. The EEG recordings of simultaneous EEG-fMRI, however, are overlaid to a great degree by fMRI related artifacts and an artifact reduction is mandatory before any EEG analysis. The most severe artifacts – the gradient artifact and the pulse artifact – are repetitive. Average artifact subtraction (AAS) technique exploits the repetitiveness and is presumably the most often used artifact reduction technique. In this method artifact templates are calculated by averaging over adjacent artifact epochs and subsequently the templates are subtracted to reduce the artifacts. Although the AAS technique is one of the best performing methods, artifact residuals are usually present in the resulting EEG after applying the AAS technique. This work aims at identifying sources of the artifact residuals.

Approach: Application of the AAS technique to artificial EEG that is contaminated with artificial fMRI related artifacts.

Main results: A new source of artifact residuals was identified. It was found that the AAS technique itself adds artifacts to the EEG during gradient artifact reduction, because the gradient artifact template is corrupted by pulse artifact remainders.

Significance: This work shows that using a standard number of 25 epochs to calculate the gradient artifact template – as suggested by the inventors of AAS – results in substantial artifact residuals and consequently to a low EEG quality. Furthermore, the work discusses how potential solutions to this problem have serious side effects such as loss of adaptivity of the AAS technique. Hence, this problem must be considered carefully already in the design of simultaneous EEG-fMRI experiments.

Introduction

In recent years electroencephalography (EEG) and functional magnetic resonance imaging (fMRI) have been applied simultaneously to study the active human brain concurrently from electrophysiological and metabolic/vascular perspectives (Ritter2006, Mulert2010, Rosa2010, Huster2012). The simultaneous application of the techniques allows the concurrent measurement of different brain signals and allows benefiting from their complementary features (Mulert2010, Rosa2010). For instance, EEG can capture signal changes in the range of milliseconds, but the exact locations of these changes remain difficult to determine (Niedermeyer2005, Michel2012). fMRI in turn can be used to determine the locations of signal changes with high precision, but the time resolution is limited to seconds (Ogawa1990, Norris2006). By combining these two techniques, the information collected with one technique can be supplemented by information from the other (Rosa2010, Mullinger2011, Huster2012, Uludag2014). One example of such an application is the EEG-informed fMRI analysis technique that is used to localize epileptic centers in the brain prior to a brain surgery (Ives1993, Krakow1999, Rosenow2001, Laufs2012).

However, EEG and fMRI are techniques that affect each other. On the one hand, the insertion of additional EEG equipment into the scanner bore results in degraded fMRI data quality, because it disturbs the magnetic field homogeneity and interferes with the radio frequency signals (Bonmassar2001, Luo2012). On the other hand, the presence of magnetic fields in MRI scanners introduce severe artifacts in the EEG. Dynamic magnetic fields induce electromagnetic force in the EEG cables according to Faraday's law. The static magnetic field of MRI scanners is also problematic, because small motions in the static magnet field – for instance by study participants – also induce significant electromagnetic force (Mullinger2008, Mulert2010). Typically, small motions cannot be avoided, because they may occur as a result of the human cardiac cycle or scanner vibrations (Bonmassar2002, Mullinger2013a, Nierhaus2013, Rothlübbers2014). Therefore, data obtained from the application of simultaneous EEG-fMRI are heavily affected by artifacts. In the case of fMRI, the data quality is reduced, but is usually sufficient to allow data analysis (Jorge2015). In the case of EEG, however, the artifacts reduce the data quality so severely that artifact reduction methods based on signal processing are strongly advised (Mullinger2013a).

Typically, two types of MRI related artifacts are dominant in the EEG and consequently, these artifacts are the main targets of artifact reduction techniques. The first type is caused by electromagnetic induction in the electrodes and the adjoining cables, due to the switching of the scanner's gradient field during the acquisition of fMRI data; this artifact type is often referred to as the gradient artifact (Yan2009). It is a broad-band artifact that covers the whole EEG relevant frequency range with amplitudes in the range of millivolts; hence, these amplitudes are roughly 1000 times higher than EEG amplitudes (Ritter2007, Mulert2010). The second artifact is mainly caused by motion of the EEG electrodes in the static magnetic field, due to cardiac-pulse-driven head nodding; this artifact type is often referred to as the pulse artifact (Debener2008, Mullinger2013b). It has maximum amplitudes of approximately 100 µV and is most prominent in the lower frequency range up to 30 Hz (Debener2008, Mulert2010, Mullinger2013b).

Other MRI related artifacts are known, for instance, the helium pump artifact or the patient ventilation system related artifact (Nierhaus2013, Rothlübbers2014). They are caused by vibrations introduced by the helium

2

cooling system or the fans of the patient ventilation system. Although initial attempts to reduce these types of artifacts have been made, they are often not considered during the artifact reduction process, because they usually reduce data quality less than the gradient and pulse artifact and they are harder to remove due to their complex and non-repetitive structure.

A method that is often used to reduce the negative effects of the gradient artifact and the pulse artifact is the average artifact subtraction (AAS) technique (Allen1998, Allen2000). The method exploits the repetitive nature of both artifacts. An artifact template is calculated for the current artifact epoch by averaging over neighboring artifact epochs. The template is then subtracted from the current epoch to reduce the artifact. The method is typically applied twice: firstly, it is applied to reduce the effects of the gradient artifact, and secondly, to reduce the effects of the pulse artifact (Allen1998, Allen2000). The AAS technique relies on three implicit assumptions: (1) The EEG has zero mean. Hence, no EEG remains after averaging over EEG epochs. (2) The artifact is repetitive. Hence, one can partition the EEG data into artifact epochs. (3) The artifact remains constant across adjacent artifact epochs. Assumptions (1) and (2) are typically fulfilled for the gradient and pulse artifact. For instance, regarding the first assumption, one can achieve zero mean EEG by high pass filtering. Regarding assumption two, one can reliably divide the gradient artifact into epochs that are determined by the time of repetition of the MRI scanner sequence. The pulse artifact can be divided into epochs using separate simultaneously recorded ECG signals (Mullinger2008). Assumption (3), however, is problematic. Firstly, any head motions induce artifacts and can potentially alter the shape of the gradient and pulse artifact permanently. Secondly, the cardiac pulse cycle inherently varies in terms of its magnitude and timing. This violation of assumption (3) leads to the following behavior of the AAS technique. In terms of gradient artifact reduction: the higher the number of artifact epochs included, the higher is the template quality, since the remaining signals in the template are lower after averaging. However, a high number of artifact epochs also means that it takes longer to obtain a clean template again after a change in the artifact shape, for either a magnitude or timing, occurrence. Hence, this adaptivity to changes in the artifact is determined by the number of artifact epochs for averaging. In terms of pulse artifact reduction: the pulse artifact is inherently variable and a higher number of artifact epochs will not necessarily improve the template quality. However, the adaptivity of the AAS technique is still impaired by a higher number of artifact epochs. In their seminal paper on AAS for pulse artifact reduction, Allen et al. decided to include the pulse artifact epochs of 10 s of the preceding EEG signal relative to the current epoch into the averaging to construct the template (Allen1998). Later, Allen et al. adjusted the averaging procedure. In their second paper on AAS – now for gradient artifact reduction – they argued that since artifact correction is often performed offline, it is possible to include not only past artifact epochs, but also future artifact epochs in the averaging (Allen2000). Furthermore, they proposed an answer to the question of how many epochs should be included in the averaging process. They argued that signal components that occur in EEG (artifacts and brain-signals) have amplitudes of 10-250 μV and, therefore, it is necessary to include at least 25 epochs in the averaging to ensure that the residual amplitudes of the largest components in the template are below the amplitudes of smallest components in the EEG signal. By combining these two enhancements, they decided to include twelve past artifact epochs, twelve future epochs and the current artifact epoch in the calculation of the artifact template (Allen2000). The AAS technique is currently available in commercial fMRI-compatible EEG systems for the reduction of both the gradient and the pulse artifact. Examples of such systems are the BrainAmp system (BrainProducts, Mu-
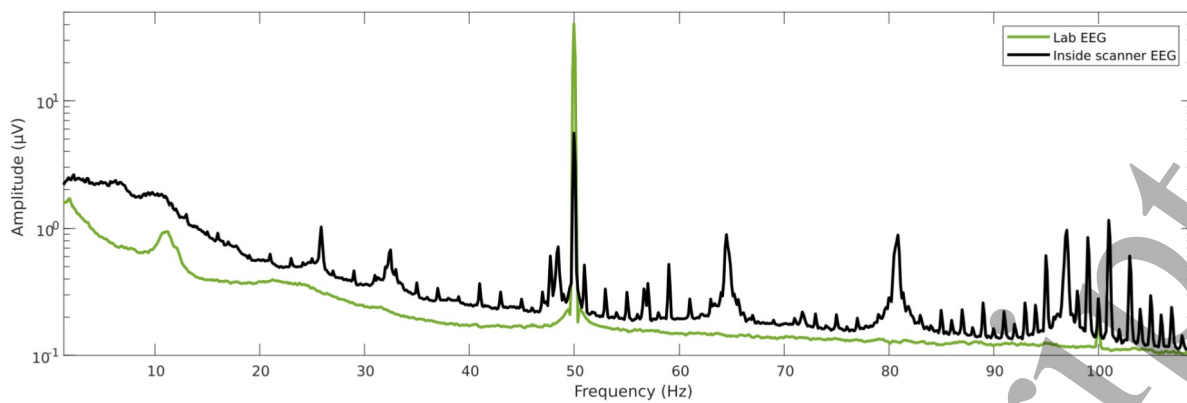
Figure 1: Spectra of EEG. Green: spectrum of EEG recorded in lab environment. Black: spectrum of EEG recorded inside the active MRI scanner after two subsequent applications of the AAS method for gradient and pulse artifact reduction. Channels with excessive power (mean ± 2 std) were excluded. The spectra were calculated with Welch's method for each EEG channel separately (500 Hz sample rate, 1 Hz high pass, 125 Hz low pass, Kaiser window, window length 8 s, overlap approximately 50%) and were subsequently averaged over 6 participants.

nich, Germany), the Geodesic EEG system (Electrical Geodesics, Inc., Eugene, OR, USA), or the NEURO PRAX system (neuroCare GmbH, Germany). However, AAS is not only used as a stand-alone technique, but is often used as a pre-processing step before other techniques. For instance, the AAS technique is deployed as part of the optimal basis sets method and before reference layer adaptive filtering (Niazy2005, Steyrl2017, Steyrl2018). Furthermore, an on-line version of AAS is also available commercially (Allen1998). Finally, it is also one of the best performing artifact reduction techniques (Garreffa2003, Grouiller2007, Ritter2007). As a result, AAS is presumably the most frequently used artifact reduction technique in simultaneous EEG-fMRI.

Nevertheless, the results of several studies have shown that EEG recorded in a lab environment is significantly different from EEG recorded inside an MRI scanner, although the AAS technique was used to reduce the gradient and pulse artifact (Benar2003, Grouiller2007, Ritter2007). An example is depicted in Figure 1. Figure 1 shows EEG spectra from the same study participants, first recorded in a lab environment and then inside an active MRI scanner with subsequent AAS. In the spectrum of EEG recorded inside the scanner, one can identify single peaks starting at around 25 Hz. These peaks seem to originate from gradient artifact residuals as well as from artifacts related to vibrations, i.e. those related to the cooling and patient ventilation systems. In addition to the artifact peaks, the amplitude of EEG recorded inside the MRI scanner is substantially higher across the frequency range from 1 Hz to approximately 40 Hz compared to the amplitude of EEG recorded in the lab. These artifact amplitudes overlay the typical peaks in the EEG spectrum that are associated with well-known and important brain rhythms; alpha rhythm at 8-13 Hz and beta rhythm at 13-30 Hz. To the best of our knowledge the cause of this broad band artifact has not yet been investigated.

Based on theoretical considerations, our hypothesis is that the AAS technique itself is a fundamental cause of this artifact. In this work, we apply the AAS technique to artificial EEG data to demonstrate that pulse artifact residuals in the AAS template during the gradient artifact reduction, add this artifact to the EEG.

Methods

An evaluation of artifact reduction techniques is problematic when artifacts and the signal of interest are available only as a mixture, as is the case with EEG of simultaneous EEG-fMRI. Inspired by a work of
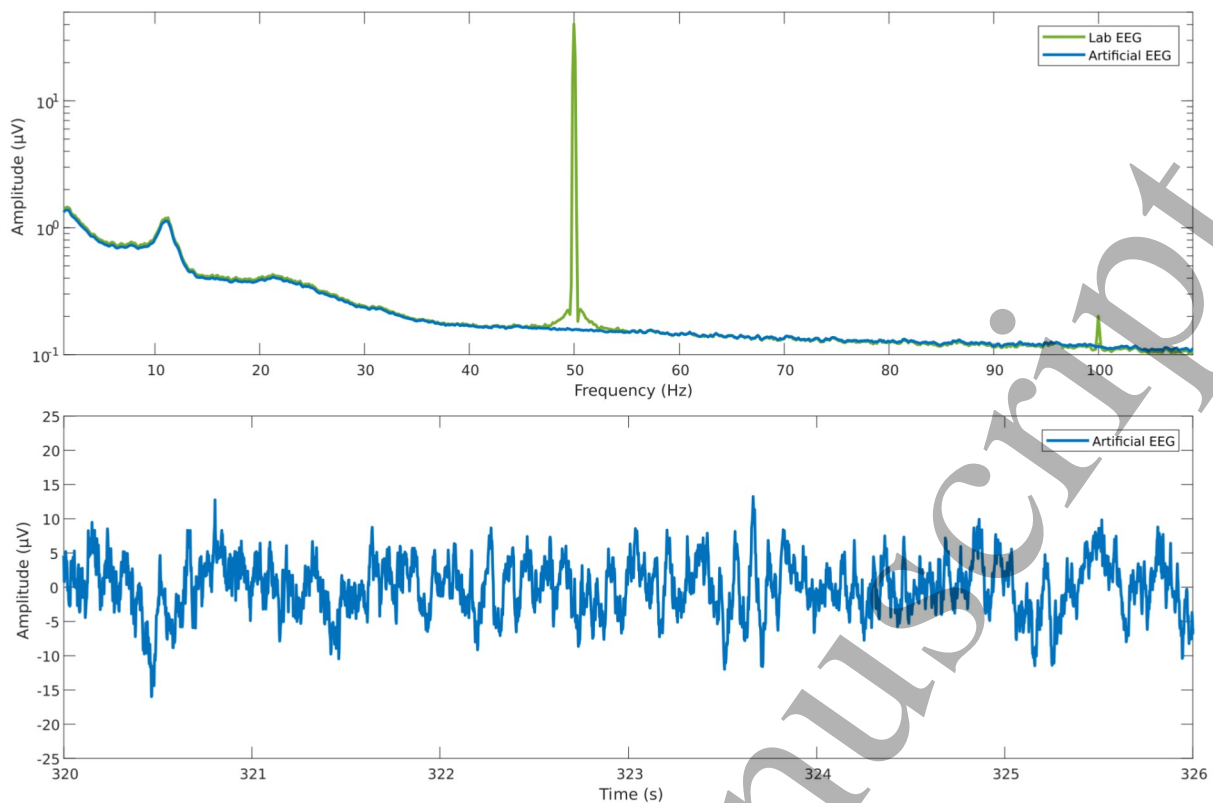
Figure 2: Top: spectrum of EEG recorded in a lab environment (green) and spectrum of the artificially generated EEG signal (blue). Bottom: example of time course of the artificial EEG signal.

Grouiller et al., we use a procedure that is based on artificial signals to avoid the mixture problem (Grouiller2007). The procedure uses a single artificial EEG channel that is built of known components. Three components are included: an artificial EEG component, an artificial gradient artifact component and an artificial pulse artifact component. The components serve as references in the evaluation. The procedure itself has three steps: (1) We generate representative artificial signal components and out of them, we create a single channel artificial EEG by summing up the components. The statistical properties of these artificial signal components are based on real simultaneous EEG-fMRI recordings from our previous work. Please refer to it for recording details (Steyrl2018). Descriptions of the component generation are presented later in this section. (2) We apply the AAS technique two times. Firstly to reduce the gradient artifact (GA-AAS) and a secondly to reduce the pulse artifact (PA-AAS). In both, we include 25 artifact epochs in the template averaging step, 12 taken from before the current epoch, 12 taken from after the current epoch, and the current epoch; as recommended by Allen et al. (Allen2000). (3) We compare the reconstructed EEG component after GA-AAS and PA-AAS with the original artificial EEG component to determine the effects of the applications of the AAS technique. Furthermore, this procedure allows the investigation of the individual steps of the AAS technique. For instance, we investigate the quality of the artifact template in GA-AAS.

Artificial EEG component

The artifact-free EEG is the signal component of interest. We want to recover this component by applying the AAS technique. In order to create a realistic, representative, single-channel, artificial EEG component, we use the average spectrum of EEG that was recorded in a lab environment, see Figure 2 top (Steyrl2018). This spectrum was calculated by averaging over all individual spectra of the EEG channels collected from 6
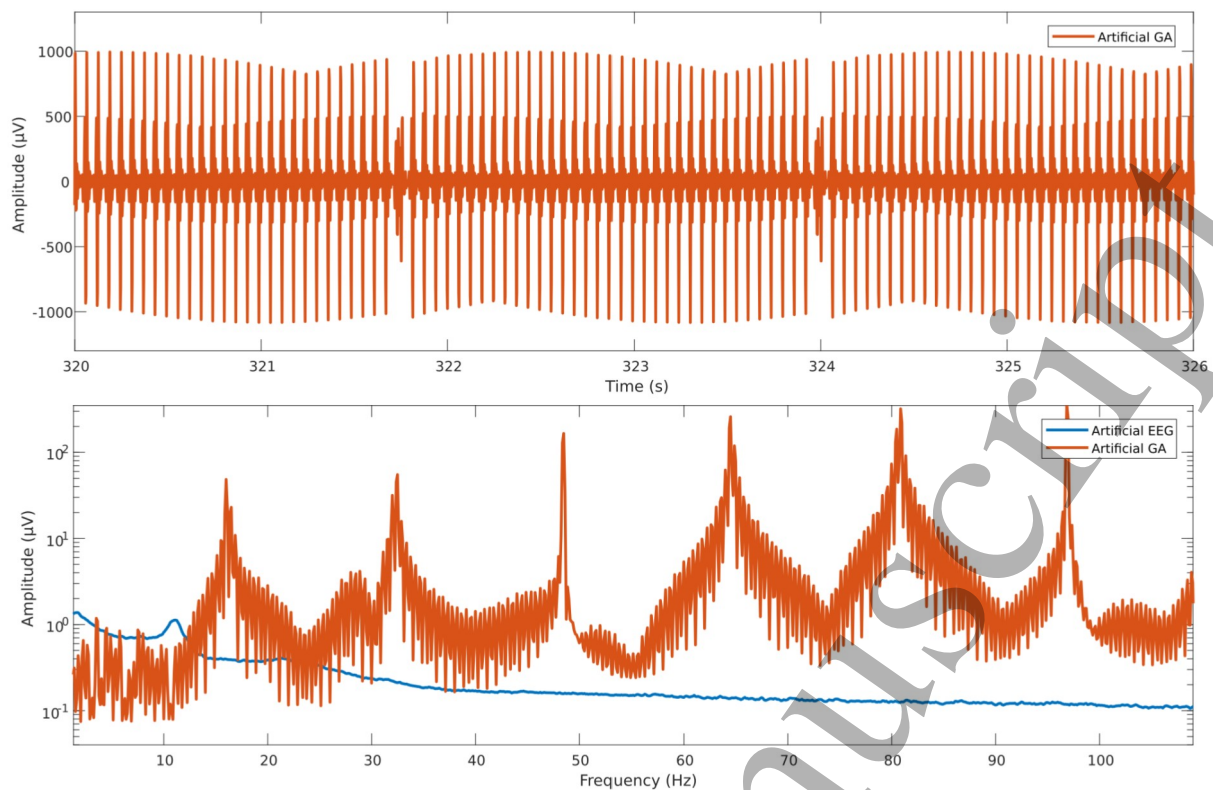
Figure 3: Top: repeated artifact template used to obtain a 2 h long artificial gradient artifact component. Bottom: comparison of spectrum of the artificial gradient artifact component (red) with that of the artificial EEG (blue).

participants. Channels with excessive power (mean ± 2 std) were excluded. The individual spectra were calculated using Welch's method (500 Hz sample rate, 1 Hz high pass, 125 Hz low pass, Kaiser window, length 16 s, overlap approximately 50%). The 50 and 100 Hz peaks were removed by interpolating the average spectrum between 45 and 55 Hz, and between 99 and 101 Hz. A new frequency axis with a frequency resolution that is 420 times higher than the frequency resolution of the average spectrum was created, and the average spectrum was interpolated to fit to this new axis. The amplitudes were adjusted to fit Rayleigh's energy theorem (Oppenheim2003). To create a time domain EEG signal from that spectrum, an inverse Fourier transform was applied to the spectrum. The result is an artificial EEG signal with a length of 2 h and a sample rate of 500 Hz (Figure 2 bottom). Its spectrum is similar to that of lab EEG (Figure 2 top).

Gradient artifact component

The gradient artifact is the most severe type of artifacts in terms of its amplitude. We chose an EEG channel with a representative gradient artifact to generate an artificial gradient artifact component (channel POz of participant 2 in Steyrl et al. 2018). The EEG channel was recorded with a sampling rate of 5000 Hz and activated synchronization between the EEG system clock and the MRI scanner clock. The time-of-repetition of the scanner was 2250 ms, an integer multiple of 20 μs. Subsequently, the EEG channel was low pass filtered to avoid aliasing (12th order, second-order-structure, zero phase Butterworth low pass filter, 3 dB at 125 Hz) and down-sampled to 500 Hz. We checked for an effect of the down-sampling on the gradient artifact reduction and found that the EEG quality was equal. The actual gradient artifact component was generated by repeating a gradient artifact template until the desired length of the component was reached. The template was obtained by averaging over gradient artifact epochs of the aforementioned EEG channel. Single gradient arti-
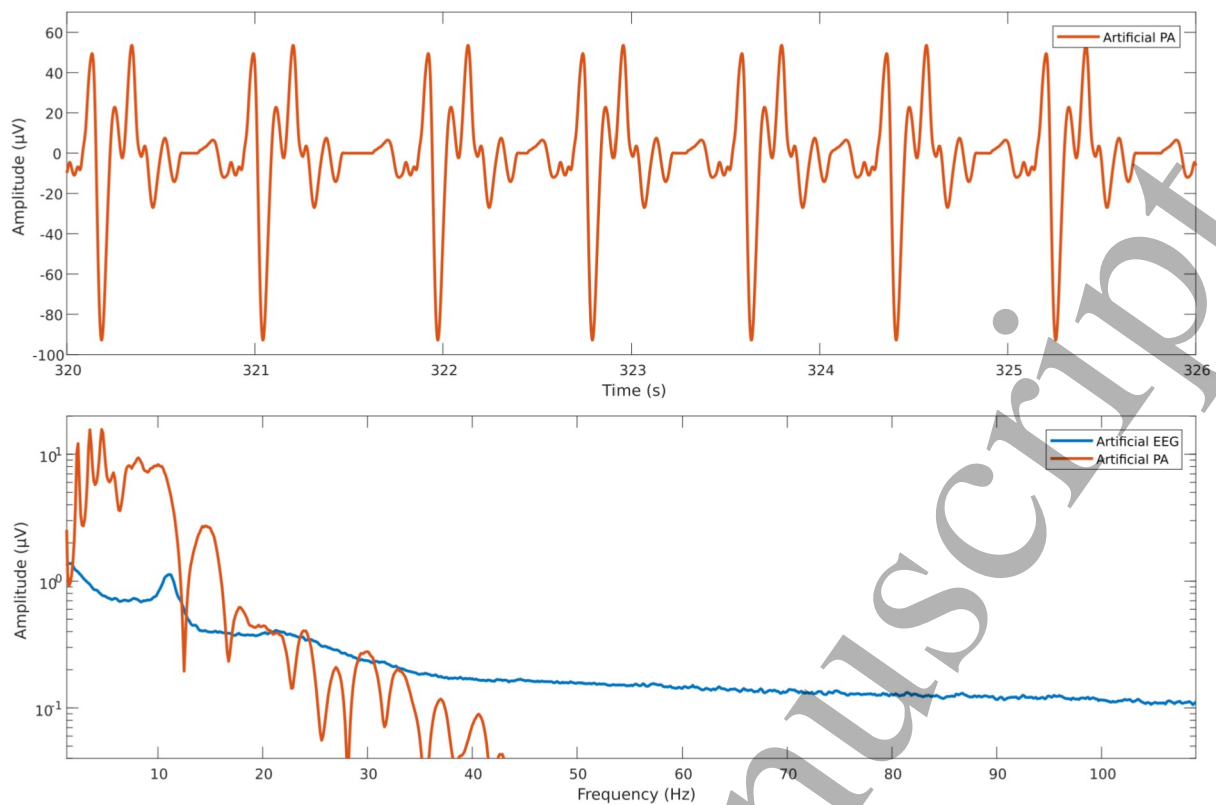
Figure 4: Top: repeated pulse artifact template to obtain a 2 h long artificial pulse artifact component. Bottom: comparison of spectrum of the artificial pulse artifact component (red) with that of the artificial EEG (blue).

fact epochs were removed before the averaging if they showed excessive power (mean ± 2 std). In total 464 gradient artifact epochs were included to calculate the gradient artifact template. The template was then repeated until a signal length of 2 h was reached (see Figure 3 top). The artificial gradient artifact component shows the typical spectral fingerprint of the gradient artifact: prominent peaks at 16 Hz, 32 Hz, 48 Hz, 64 Hz, 80 Hz, 96 Hz (see Figure 3 bottom). We decided to carry out our investigations under conditions that are optimal for the AAS technique, hence, the artificial gradient artifact component does not include any abrupt or slow changes over its entire duration.

Pulse artifact component

To create an artificial pulse artifact component, we used a similar approach as that for the gradient artifact component. Pulse artifact epochs of an EEG channel that shows representative pulse artifacts (channel POz of participant 2 in Steyrl2018) were averaged to obtain a pulse artifact template. Epochs with excessive power (mean ± 2 std) were removed. In total 914 pulse artifact epochs were included to calculate the pulse artifact template. To obtain an artificial 2 h pulse artifact signal, we lined up one artifact after another, but the duration between two successive artifacts was varied, to simulate the natural temporal variability of the pulse artifact occurrence. The gaps in between adjacent artifact epochs were filled with zeros. We adjusted the pulse artifact occurrence to match the measured average heart rate of participant 2 (see Figure 4 top). On average, a pulse artifact occurred every 0.86 s, which implied a heart rate of approximately 70 bpm. The standard deviation was 0.05 s. The artificial pulse artifact component shows the typical spectral signature of the pulse artifact: high power in the frequency range of 1 to 40 Hz and almost no power above 40 Hz. The

pulse artifact amplitude was not modified over the course of the artificial pulse artifact component to ensure optimal conditions for AAS.

Performance metrics

We present a visual (time and frequency domain) comparison of the artificial EEG component, the reconstructed EEG after twice applying AAS (GA-AAS and PA-AAS), the artifact residuals in the reconstructed EEG, and the artifact residuals in the gradient artifact template. The artifact residuals of the reconstructed EEG were obtained by subtracting the artificial EEG component from the reconstructed EEG. The artifact residuals in the gradient artifact template were obtained by subtracting the gradient artifact component from the template.

A helpful metric that can be used to assess the similarity of signals is the Pearson correlation coefficient. This coefficient describes the difference between the original artificial EEG components and the reconstructed EEG component in the time domain; ideally, this coefficient is 1, implying that the signals are identical.

Furthermore, we calculate the signal-to-noise ratio (SNR) between the artificial EEG component and the artifact residuals in the reconstructed EEG to quantify the quality loss.

Computations were performed with Matlab (Mathworks Inc., Natick, MA, USA, Version 2017b).

Results

Figure 5 shows a representative period of: the artificial EEG component, the reconstructed EEG after GA-AAS and PA-AAS, the artifact residuals in the reconstructed EEG, and the artifact residuals in the gradient artifact template. The Pearson correlation coefficient between the artificial EEG component and the reconstructed EEG after two times AAS is 0.6. The SNR between the artificial EEG component and the artifact residuals in the reconstructed EEG is - 1.8 dB. The correlation coefficient between the residuals in the reconstructed EEG and the residuals in the gradient artifact template is 0.94.

Figure 6 presents the spectra of: the artificial EEG component, the reconstructed EEG after GA-AAS and PA-AAS, the artifact residuals in the reconstructed EEG, and the artifact residuals in the gradient artifact template.

Discussion

Artifact reduction techniques are strongly advised as a rule prior to any analysis of EEG that was obtained during simultaneous EEG-fMRI. The artifacts represent a major problem for the analysis of the EEG, especially when oscillatory EEG components are under investigation or when only a small number of event-related potential are available (Steyrl2013, Zich2015).

The AAS technique is one of the most frequently applied methods for artifact reduction and also one of the best performing compared to other available artifact reduction methods (Grouiller2007). Nevertheless, some of the commonly investigated brain rhythms are typically masked by remaining artifacts appearing in the
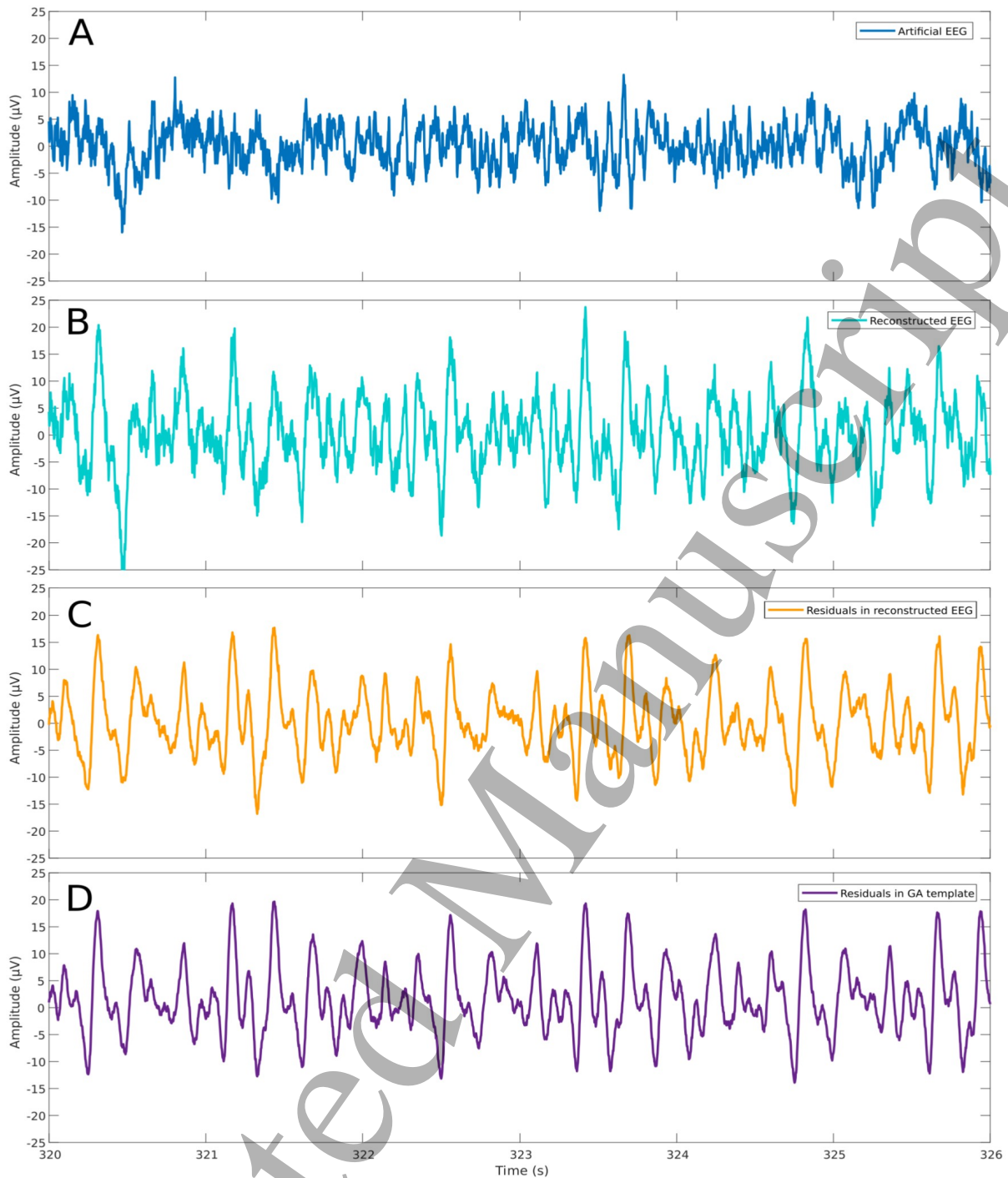
8

Figure 5: Comparison of: the artificial EEG component (A), the reconstructed EEG after two times AAS (GA-AAS and PA-AAS) (B), the artifact residuals in the reconstructed EEG (C), and the artifact residuals in the gradient artifact template (D).

EEG although artifact reduction methods were applied. It is clear that some of these remaining artifacts are of a type that require a different reduction method, e.g. artifacts related to vibrations, as the helium pump arti-fact (Mullinger2013a, Rothlübbers2014). It is also clear, however, that artifact residuals of the gradient and the pulse artifact are still present after artifact reduction (Figure 1). Therefore, the question is: why is the AAS technique not able to completely remove the artifacts for which it was developed? One answer is that the as-sumption on the similarity of adjacent artifact epochs is violated, meaning that adjacent artifact epochs do not have the same timing and amplitude. In the case of the gradient artifact, small head motions change the shape of artifact epochs and leads to the introduction of gradient artifact residuals in the data (Yan2009). In
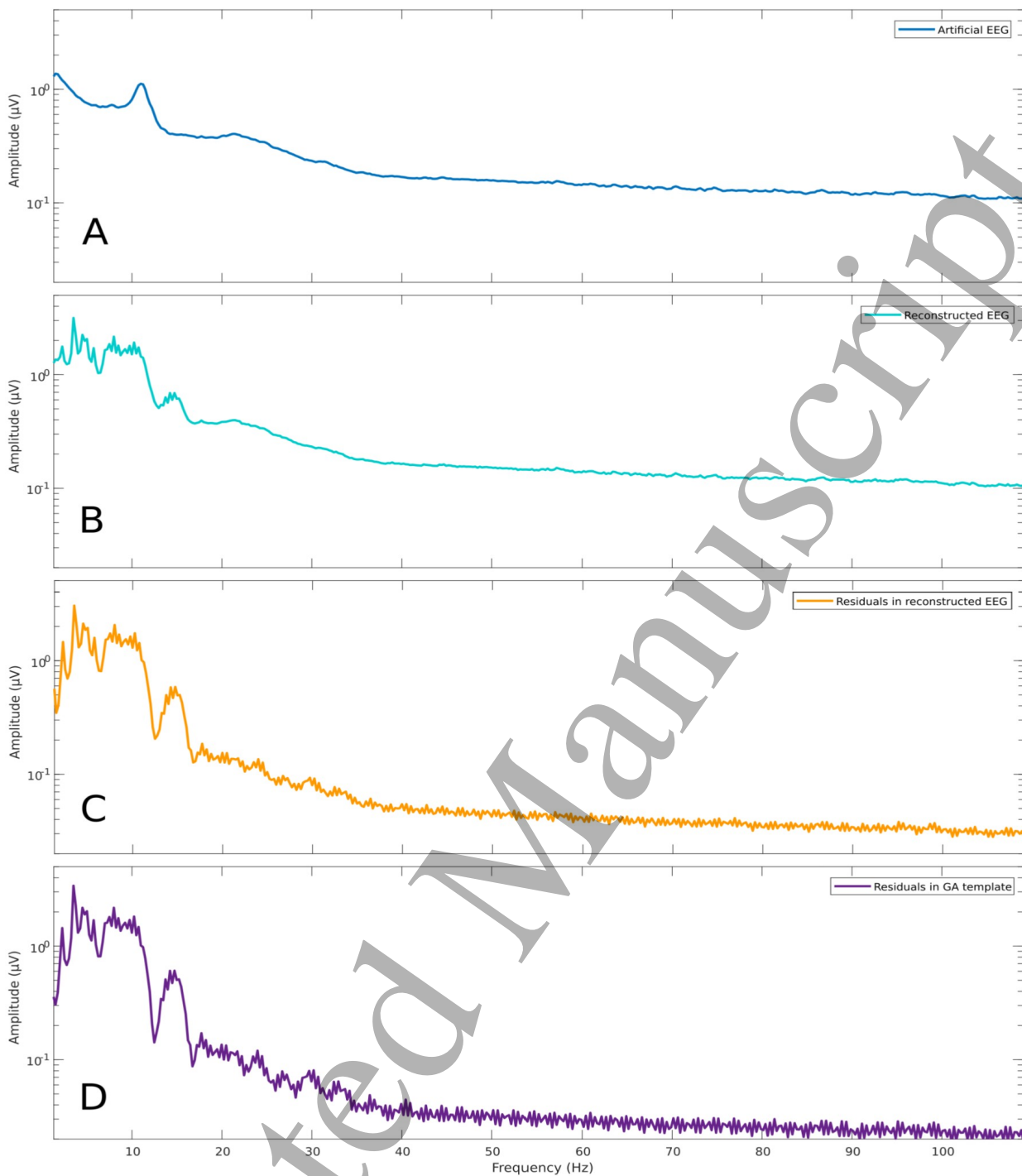
Figure 6: Comparison of the spectra of: the artificial EEG component (A), the reconstructed EEG after two times AAS (GA-AAS and PA-AAS) (B), the artifact residuals in the reconstructed EEG (C), and the artifact residuals in the gradient artifact template (D).

the case of the pulse artifact, the violation of the similarity assumption is even worse as this artifact is inherently variable and calculated templates are only approximations of the artifact epochs (Mullinger2013b).

In this study, however, we created perfect conditions for the AAS technique in terms of gradient and pulse artifact reduction, because we constructed data without any artifact variation or additional artifacts as eye blink artifacts or power line artifacts. Nonetheless, we can still observe severe artifact residuals in the reconstructed EEG after the application of GA-AAS and PA-AAS. The reconstructed EEG clearly differs from the original artificial EEG in both, time and frequency domain (compare Figure 5 A, Figure 5 B and Figure 6 A,

Figure 6 B). This impression is supported by the only moderate correlation coefficient of 0.6 between the artificial EEG and the reconstructed EEG. Furthermore, the SNR between the artificial EEG and the artifact residuals in the reconstructed EEG is -1.6 dB only. This negative SNR implies that the artifact residuals (Figure 5 C and Figure 6 C) are greater than the artificial EEG component, which explains the observation that important brain rhythms as the alpha rhythm are often not visible in EEG obtained during fMRI. These results are highly problematic since for EEG analysis we usually assume a correlation of near 1 and a high SNR, since we expect that the reconstructed EEG is the real EEG and draw our conclusions based on this assumption.

One example: The artifact residuals cover the alpha rhythm in the EEG. Although it is still possible to analyze the differences in alpha rhythm between two settings, the absolute amplitude cannot be used anymore.

Cause of the residual artifacts

A comparison of the spectral signatures of the pulse artifact (Figure 4 bottom) with the residual artifacts in the reconstructed EEG (Figure 6 C) indicates that the residual artifacts are remainders of the pulse artifact. Furthermore, the artifact residuals in the gradient artifact template during GA-AAS (Figure 5 D, Figure 6 D) are very similar to those in the reconstructed EEG in time domain as well as in frequency domain. For instance, their correlation coefficient in time domain is 0.95. Hence, pulse artifact remainders are present in the gradient artifact template and consequently, the remainders are added to the reconstructed EEG during gradient artifact template subtraction. Consequently, template corruption is indeed the cause of the artifact residuals in the reconstructed EEG. The pulse artifact component in our study has a maximum amplitude of about 100 µV. According to Allen et al. averaging over 25 epochs should reduce this amplitude to about 4 µV in the template (Allen2000). However, about three pulse artifact epochs are present in every epoch of the gradient artifact. These single pulse artifact epochs may add up with the pulse artifact epochs of other gradient artifact epochs during the gradient artifact template construction, because they are aligned by chance during averaging. This increases the residual pulse artifact observed in the template by the number of aligned artifacts. We observed residual pulse artifact amplitudes of up to 20 µV instead of the expected residual pulse artifact amplitudes of about 4 µV.

Allen et al. suggested the use of 25 artifact epochs to calculate the artifact templates (Allen2000). Their reason for that number was that 25 epochs should be enough to reduce artifact residuals in the template to be smaller than the EEG component of interest. However, the number of 25 epochs holds only for single artifacts, for instance eye blinks, but it does not hold for repetitive artifacts, if they are correlated – at least temporarily – with the gradient artifact epochs. During GA-AAS, pulse artifacts are present in every single gradient artifact epoch; therefore, the residual pulse artifact amplitudes in the gradient artifact template are reduced by approximately a factor of square-root of the number of the epochs and not by the number of the epochs. Hence, using 25 epochs in the averaging step implies that pulse artifact amplitudes in the gradient artifact template are reduced by a factor of $\sqrt{25}$ (i.e., only by a factor of 5) and this leads to the residual pulse artifact amplitudes of up to 20 µV in the reconstructed EEG.

Reducing pulse artifact residuals in the gradient artifact template by higher numbers of epochs

Theoretically, an obvious solution of the problem of the pulse artifact residuals in the gradient artifact template is to use more gradient artifact epochs in the template construction process during GA-AAS. For instance, we tested 101 gradient artifact epochs and found a substantial reduction of pulse artifact residuals. The correlation coefficient of artificial EEG and reconstructed EEG improved to 0.84. The SNR of artificial EEG and residual artifacts in the reconstructed EEG improved to 3.8 dB. However, the increased number of gradient artifact epochs reduces the adaptivity of the AAS technique. For example, 101 epochs and a scanner time-of-repetition of 2.5 s implies that 4.2 minutes of EEG are included in the averaging for the template creation. Hence, if motion occurs during that time, all templates that include the gradient artifact epochs in which the motion occurs will be distorted. Consequently, in real AAS applications with motions of the study participants, the quality of the artifact template would increase with the number of epochs up to a certain point and then degrade again. One could formulate this situation as an optimization problem, dependent on the frequency of the motion. However, an individual optimization step per study participant would be necessary, which may be impracticable.

Variant of AAS

Interestingly, modifications of the AAS technique that aim at improving the template quality have already been proposed. Sijbers et al. suggested using median filtering instead of averaging for the template creation (Sijbers2000). The median filtering should mitigate the effects of artifacts in the template. Our experience, however, is that this method is somewhat advantageous in the lower frequency range, but increases the gradient artifact residuals in the upper frequency range and as a result we found no overall benefit.

Gonçalves et al. proposed another modification: weighting epochs by their variance in the averaging step (Gonçalves2007). The idea behind this approach is that the artifact affected EEG epochs have a higher variance than those without artifacts. This method is possibly beneficial if single artifacts are present, but we identified the pulse artifact as the main contributor to the artifact residuals in the template. The pulse artifact is present at all times and constantly contributes to the variance. Therefore, the weighting step has virtually no influence on the pulse artifact residuals found in the gradient artifact template.

Post AAS techniques to improve EEG quality

In addition to improving the AAS technique, a further option is to use additional artifact reduction methods after the AAS technique to improve the EEG quality. Different methods were proposed. One example is that of linear signal decomposition based techniques. For instance, temporal principal component analysis can be applied to find and remove residual of the gradient and pulse artifact in the reconstructed EEG (Niazy2005). This method is known as optimal basis sets technique and it seems that in comparison to the AAS technique, it is beneficial for lower sampling rates, but less effective for interictal spikes reconstruction (Grouiller2007). Other linear signal decomposition techniques are spatial principal component analysis or independent component analysis (Benar2003, Srivastava2005). However, we agree with Niazy et al. who have already pointed out that: "*One problem with these approaches is that they necessitate the presence of a large num-*

12

ber of sensors. Also, the identification of artifact components can be subjective and is usually done manually. Most importantly, spatial filters assume that all the sensors are contaminated by common sources, which is not the case. The BCG artifact [pulse artifact] *derives from sources that are rotating/moving, which contaminate different sensors at different points during the cardiac cycle with different effects.*" (Niazy2005). A different approach to improve the EEG quality is based on adaptive filtering. Independent recordings of the artifacts or the artifact residuals are used as input for an adaptive filter to reduce the artifact residuals further. This approach showed very promising results, but additional hardware – as yet often only available in prototype – is necessary and is therefore a limiting factor for this approach (Bonmassar2002, Masterton2007, Abbott2014, Steyrl2017, Steyrl2018).

Conclusions

Our results reveal a previously unknown source of artifact residuals in EEG of simultaneous EEG-fMRI. The AAS technique itself adds artifact residuals to the EEG, although we created optimal conditions for the AAS technique. In particular, pulse artifact residuals that remain in the gradient artifact template are added to the reconstructed EEG. The artifact residuals mask the commonly analyzed alpha and beta rhythms of the EEG. Therefore, researchers should be aware that the AAS method can substantially contaminate the EEG data. In theory, the pulse artifact residuals in the gradient artifact template can be reduced by using a higher number of gradient artifact epochs in the averaging procedure. However, this comes at the cost of adaptivity of the AAS technique. Adaptivity is important in real AAS applications, where study participants move their heads. The optimal number of epochs for the template calculation is thus difficult to define. However, using 25 epochs in the averaging step, as suggested by Allen et al., results in a low EEG quality. Post-processing techniques, e.g. adaptive filters based techniques, can be deployed to potentially improve the EEG quality.

Acknowledgments

References

[Abbott2014] Abbott D.F., Masterton R. A.J., Archer J.S., Fleming S.W., Warren A.E.L., Jackson G.D., 2014. Constructing Carbon Fiber Motion-Detection Loops for Simultaneous EEG–fMRI. Frontiers in Neurology, 5, 260. doi:10.3389/fneur.2014.00260

[Allen1998] Allen P.J., Polizzi G., Krakow K., Fish D.R., Lemieux L. 1998. Identification of EEG events in the MR scanner: the problem of pulse artifact and a method for its subtraction. Neuroimage, 8(3), pp.229-239. doi:10.1006/nimg.1998.0361

[Allen2000] Allen P.J., Josephs O., and Turner R., 2000. A method for removing imaging artifact from continuous EEG recorded during functional MRI. Neuroimage, 12(2), pp.230-239. doi:10.1006/nimg.2000.0599

[Benar2003] Christian-G Bénar, Yahya Aghakhani, Yunhua Wang, Aaron Izenberg, Abdullah Al-Asmi, François Dubeau, and Jean Gotman, 2003, Quality of EEG in simultaneous EEG-fMRI for epilepsy, Clinical Neurophysiology, vol.114(3), pp.569-580. doi:10.1016/S1388-2457(02)00383-8

[Bonmassar2001] Bonmassar G., Hadjikhani N., Ives J. R., Hinton D., Belliveau J. W., 2010. Influence of EEG electrodes on the BOLD fMRI signal. Hum Brain Mapp, 14, pp.108-115. doi:10.1002/hbm.1045

[Bonmassar2002] Bonmassar G., Purdon P.L., Jääskeläinen I.P., Chiappa K., Solo V., Brown E.N., Belliveau J.W., 2002. Motion and Ballistocardiogram Artifact Removal for Interleaved Recording of EEG and EPs during MRI. NeuroImage, 16, pp.1127-1141. doi:10.1006/nimg.2002.1125

[Debener2008] Debener S., Mullinger K.J., Niazy R.K., Bowtell R.W., 2008. Properties of the ballistocardiogram artefact as revealed by EEG recordings at 1.5, 3 and 7 Tesla static magnetic field strength. Int. J. Psychophysiol., 67(3), pp.189-199. doi:10.1016/j.ijpsycho.2007.05.015

[Garreffa2003] G. Garreffa, M. Carnì, G. Gualniera, G.B. Ricci, L. Bozzao, D. De Carli, P. Morasso, P. Pantano, C. Colonnese, V. Roma, B. Maraviglia, 2003, Real-time MR artifacts filtering during continuous EEG/fMRI acquisition. Magnetic Resonance Imaging, vol.21(10), pp.1175-1189. doi:10.1016/j.mri.2003.08.019

[Gonçalves2007] S. I. Gonçalves, P. J. W. Pouwels, J. P. A. Kuijer, R. M. Heethaar, J. C. de Munck, 2007, Artifact removal in co-registered EEG/fMRI by selective average subtraction, Clinical Neurophysiology, vol.118(11), pp.2437-2450. doi:10.1016/j.clinph.2007.08.017

[Grouiller2007] Frédéric Grouiller, Laurent Vercueil, Alexandre Krainik, Christoph Segebarth, Philippe Kahane, and Olivier David, 2007, A comparative study of different artefact removal algorithms for EEG signals acquired during functional MRI, NeuroImage, vol.38, pp.124-137. doi:10.1016/j.neuroimage.2007.07.025

[Huster2012] Huster R.J., Debener S., Eichele T., Herrmann C.S., 2012. Methods for simultaneous EEG-fMRI: an introductory review. The Journal of neuroscience, 32(18), pp.6053-6060. doi: 10.1523/JNEUROSCI.0447-12.2012

[Ives1993] J. R. Ives, S. Warach, F. Schmitt, R. R. Edelman, and D. L. Schomer, 1993, Monitoring the patient's EEG during echo planar MRI, Electroencephalography and Clinical Neurophysiology, vol.87(6), pp.417-420. Doi:10.1016/0013-4694(93)90156-P

[Jorge2015] Jorge J., Grouiller F., Ipek Ö., Stoermer R., Michel C.M., Figueiredo P., van der Zwaag W., Gruetter R., 2015. Simultaneous EEG-fMRI at ultra-high field: Artifact prevention and safety assessment. NeuroImage, 105, pp.132-144. doi:10.1016/j.neuroimage.2014.10.055

[Krakow1999] K. Krakow, F. G. Woermann, M. R. Symms, P. J. Allen, L. Lemieux, G. J. Barker, J. S. Duncan, and D. R. Fish, 1999, EEG-triggered functional MRI of interictal epileptiform activity in patients with partial seizures, Brain, vol.122(9), pp.1679–1688. doi:10.1093/brain/122.9.1679

[Laufs2012] Laufs H., 2012. A personalized history of EEG–fMRI integration. NeuroImage 62, pp.1056–1067. doi:10.1016/j.neuroimage.2012.01.039

[Luo2012] Luo Q., Glover G.H., 2012. Influence of dense-array EEG cap on fMRI signal. Magn Reson Med, 68, pp.807-815. doi: 10.1002/mrm.23299

[Masterton2007] Masterton R.A., Abbott D.F., Fleming S.W., Jackson G.D., 2007. Measurement and reduction of motion and ballistocardiogram artefacts from simultaneous EEG and fMRI recordings. Neuroimage, 37, 202–211. doi:10.1016/j.neuroimage.2007.02.060

[Michel2012] Michel C.M., Murray M.M., 2012. Towards the utilization of EEG as a brain imaging tool. *NeuroImage, 61*, pp.371-385. doi:10.1016/j.neuroimage.2011.12.039

[Mulert2010] Mulert C., Lemieux L., 2010. EEG-fMRI Physiological Basics, Technique, and Applications, Springer Heidelberg Dordrecht London New York, ISBN:978-3-540-87918-3, doi:10.1007/978-3-540-87919-0

[Mullinger2008] Mullinger K.J., Morgan P.S., Bowtell R.W., 2008. Improved Artifact Correction for Combined Electroencephalography/Functional MRI by Means of Synchronization and Use of Vectorcardiogram Recordings. Journal of Magnetic Resonance Imaging, 27, pp.607-616. doi:10.1002/jmri.21277

[Mullinger2011] Mullinger K.J., Bowtell R., 2011. Combining EEG and fMRI. In M. Modo, J.W.M. Bulte (eds.), Magnetic Resonance Neuroimaging, Methods in Molecular Biology 711, Springer Science+Business Media, pp.303-326. doi:10.1007/978-1-61737-992-5_15

[Mullinger2013a] Mullinger K.J., Castellone P., Richard Bowtell R., 2013. Best Current Practice for Obtaining High Quality EEG Data During Simultaneous fMRI. Journal of Visualized Experiments : JoVE 76, 50283. PMC. Web. 2 Feb. 2016. doi:10.3791/50283

[Mullinger2013b] Mullinger K.J., Havenhand J., Bowtell R., 2013. Identifying the sources of the pulse artefact in EEG recordings made inside an MR scanner. Neuroimage, 7, pp.75-83. doi:10.1016/j.neuroimage.2012.12.070

[Niazy2005] Niazy R.K., Beckmann C.F., Iannetti G.D., Brady J.M., Smith S.M., 2005. Removal of FMRI environment artifacts from EEG data using optimal basis sets. *Neuroimage, 28*(3), pp.720-737. doi:10.1016/j.neuroimage.2005.06.067

[Niedermeyer2005] Niedermeyer E., Lopes da Silva, F.H., 2005. Electroencephalography: Basic Principles, Clinical Applications, and Related Fields, 5th ed. Lippincott Williams & Wilkins, Philadelphia. ISBN-13: 978-0781789424

[Nierhaus2013] Nierhaus T., Gundlach C., Goltz D., Thiel S.D., Pleger B., Villringer A., 2013. Internal ventilation system of MR scanners induces specific EEG artifact during simultaneous EEG-fMRI. Neuroimage, 74, pp.70-76. doi: 10.1016/j.neuroimage.2013.02.016

[Norris2006] Norris D.G., 2006. Principles of magnetic resonance assessment of brain function. *J. Magn. Reson. Imaging, 23*, pp.794-807. doi:10.1002/jmri.20587

[Ogawa1990] Ogawa S., Lee T.M., Kay A.R., Tank D.W., 1990. Brain magnetic resonance imaging with contrast dependent on blood oxygenation. Proc. Natl. Acad. Sci. U. S. A. 87, pp.9868–9872.

[Oppenheim2003] A. V. Oppenheim, and R. W. Schafer, 2003, Discrete-Time Signal Processing (3nd Ed.). Prentice-Hall, Inc., Upper Saddle River, NJ, USA. ISBN:0131988425 9780131988422

[Ritter2006] Ritter P., and Villringer A., 2006. Simultaneous EEG-fMRI. Neurosci. Biobehav. Rev., 30(6), pp.823-838. doi:10.1016/j.neubiorev.2006.06.008

[Ritter2007] Ritter P., Becker R., Graefe C., Villringer A., 2007. Evaluating gradient artifact correction of EEG data acquired simultaneously with fMRI, Magnetic Resonance Imaging, 25(6), pp.923-932. doi:10.1016/j.mri.2007.03.005

[Rosa2010] M. J. Rosa, J. Daunizeau, and K. J. Friston, 2010, EEG-fMRI integration: A critical review of biophysical modeling and data analysis approaches, Journal of Integrative Neuroscience, vol.9(4), pp. 453-476. doi: 10.1142/S0219635210002512

[Rosenow2001] Felix Rosenow, and Hans Lüders, 2001, Presurgical evaluation of epilepsy, Brain, vol.124(9), pp.1683–1700, doi:10.1093/brain/124.9.1683

[Rothlübbers2014] Rothlübbers S., Relvas V., Leal A., Murta T., Lemieux L., Figueiredo P., 2014. Characterisation and Reduction of the EEG Artefact Caused by the Helium Cooling Pump in the MR Environment: Validation in Epilepsy Patient Data, Brain Topography, vol.28(2), pp.208-220. doi:10.1007/s10548-014-0408-0

[Sijbers2000] J. Sijbers, J. Van Audekerke, M. Verhoye, A. Van der Linden, and D. Van Dyck, 2000, Reduction of ECG and gradient related artifacts in simultaneously recorded human EEG/MRI data, Magnetic Resonance Imaging, vol.18(7), pp.881-886. doi:10.1016/S0730-725X(00)00178-8

[Srivastava2005] G. Srivastava, S. Crottaz-Herbette, K. M. Lau, G. H. Glover, and V. Menon, 2005, ICA-based procedures for removing ballistocardiogram artifacts from EEG data acquired in the MRI scanner. NeuroImage, vol.24(1), pp.50-60. doi:10.1016/j.neuroimage.2004.09.041

[Steyrl2013] Steyrl D, Wriessnegger SC, Müller-Putz GR, 2013, Single trial Motor Imagery classification in EEG measured during fMRI image acquisition – a first glance. Biomedical Engineering / Biomedizinische Technik 58(Suppl.1):1-2. https://doi.org/10.1515/bmt-2013-4450

[Steyrl2017] Steyrl D, Krausz G, Koschutnig K, Edlinger G, and Müller-Putz GR, 2017, Reference layer adaptive filtering (RLAF) for EEG artifact reduction in simultaneous EEG-fMRI, Journal of Neural Engineering, vol.14(2), pp.1-20, 2017. doi:10.1088/1741-2552/14/2/026003

[Steyrl2018] Steyrl D, Krausz G, Koschutnig K, Edlinger G, and Müller-Putz GR, 2018, Online reduction of artifacts in EEG of simultaneous EEG-fMRI using reference layer adaptive filtering (RLAF), Brain Topography, vol.31(1), pp.129-149, 2018. doi:10.1007/s10548-017-0606-7

[Uludag2014] Uludag K., Roebroeck A., 2014. General overview on the merits of multimodal neuroimaging data fusion. Neuroimage, 102, pp.3-10. doi:10.1016/j.neuroimage.2014.05.018

[Yan2009] Winston X. Yan, Karen J. Mullinger, Matt J. Brookes, Richard Bowtell, 2009, Understanding gradient artefacts in simultaneous EEG/fMRI, NeuroImage, vol.46(2), pp.459-471, 2009. doi:10.1016/j.neuroimage.2009.01.029

[Zich2015] Zich C, Debener S, Kranczioch C, Bleichner MG, Gutberlet I, De Vos M, 2015, Real-time EEG feedback during simultaneous EEG-fMRI identifies the cortical signature of motor imagery. NeuroImage 114:438-447. https://doi.org/10.1016/j.neuroimage.2015.04.020

16